HHS Public Access

Author manuscript

ACS Chem Neurosci. Author manuscript; available in PMC 2019 January 22.

Published in final edited form as:

ACS Chem Neurosci. 2018 May 16; 9(5): 925–934. doi:10.1021/acschemneuro.7b00320.

Toward Serotonin Fluorescent False Neurotransmitters: Development of Fluorescent Dual Serotonin and Vesicular Monoamine Transporter Substrates for Visualizing Serotonin Neurons

Adam Henke[#1], **Yekaterina Kovalyova**[1], **Matthew Dunn**[#1], **Dominik Dreier**[1], **Niko G. Gubernator**[1], **Iva Dincheva**[2], **Christopher Hwu**[1], **Peter Šebej**[1], **Mark S. Ansorge**[2], **David Sulzer**[2,3,4], and **Dalibor Sames**[1]

[1]Department of Chemistry, and Neuro Technology Center at Columbia University, New York, NY 10027, USA.

[2]Department of Psychiatry, Columbia University, New York, NY 10032, USA.

[3]Department of Neurology, Columbia University, New York, NY 10032, USA.

[4]Department of Pharmacology, Columbia University, New York, NY 10032, USA.

[#] These authors contributed equally to this work.

Abstract

Ongoing efforts in our laboratories focus on design of optical reporters known as fluorescent false neurotransmitters (FFNs) that enable the visualization of uptake into, packaging within, and release from individual monoaminergic neurons and presynaptic sites in the brain. Here, we introduce the molecular probe FFN246 as an expansion of the FFN platform to the serotonergic system. Combining the acridone fluorophore with the ethylamine recognition element of serotonin, we identified FFN54 and FFN246 as substrates for both the serotonin transporter and the vesicular monoamine transporter 2 (VMAT2). A systematic structure-activity study revealed the basic structural chemotype of aminoalkyl acridones required for SERT activity, and enabled lowering the background labeling of these probes while maintaining SERT activity, which proved essential for obtaining sufficient signal in the brain tissue (FFN246). We demonstrate the utility of FFN246 for direct examination of SERT activity and SERT inhibitors in 96-well cell culture assays, as well as specific labeling of serotonergic neurons of the dorsal raphe nucleus in the living tissue of acute mouse brain slices. While we found only minor FFN246 accumulation in

Corresponding authors: ds43@columbia.edu and sames@chem.columbia.edu.

AUTHOR CONTRIBUTIONS

A.H., Y.K., M.D. contributed equally. N.G.G. performed the original synthesis and evaluation of FFN54. A.H. conducted screening of compounds in cell culture, as well as the design and synthesis of FFN246. A.H., D.D., and P.Š. synthesized the library of analogs. Y.K., with help from C.H., conducted follow-up cell culture experiments and quantification of uptake. I.D. and M.S.A. prepared and genotyped the animals. M.D conducted all testing and imaging of FFNs in acute mouse brain slices. A.H., Y.K., and M.D. analyzed data. Y.K. and M.D. wrote the paper, with important contributions from A.H., M.S.A., D. Sulzer, and D. Sames. D. Sames designed FFN54 and guided the design of FFN246.

The authors declare no competing financial interests.

SUPPORTING INFORMATION

Supplemental Figures S1-S4.

Probe synthesis, including detailed synthetic protocols and spectral characterization of compounds.

serotonergic axons in murine brain tissue, FFN246 effectively traces serotonin uptake and packaging in the soma of serotonergic neurons with improved photophysical properties and loading parameters compared to known serotonin-based fluorescent tracers.

Graphical Abstract

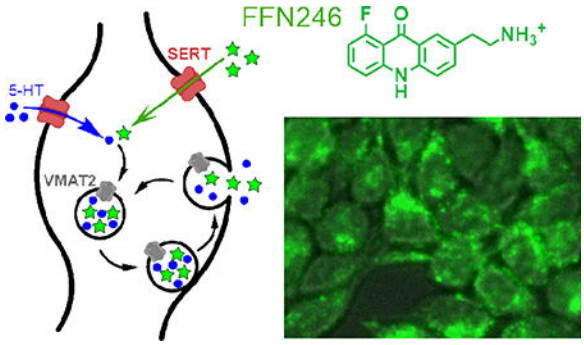

Keywords

FFN246; fluorescent false neurotransmitters; serotonin; 5-HT; monoaminergic neurons; imaging probe

INTRODUCTION

Serotonin (5-hydroxytryptamine, 5-HT) is a monoamine neurotransmitter that plays an important role in the central nervous system (CNS) and periphery. In the brain, serotonergic neurons of the raphe nuclei are primarily responsible for 5-HT neurotransmission.[1] The axonal projections of these neurons extend throughout the brain, with especially dense innervation of the cerebral cortex.[2] 5-HT neurotransmission has been implicated in the regulation of multiple human behaviors, including sleep, mood, aggression, sexuality, and addiction.[3] In the periphery, it is found at very high levels in the gastrointestinal tract[4] and plasma, where it is accumulated in blood platelets.[5] Dysregulation of 5-HT signaling has been implicated in many disorders, including mood disorders (notably depression and social anxiety disorder[6]), irritable bowel syndrome, cardiac abnormalities (e.g., cardiac valvulopathy), and platelet aggregation dysregulation.[3]

A key protein involved in regulating 5-HT neurotransmission is the plasma membrane serotonin transporter (SERT), which is largely responsible for determining the strength and duration of a 5-HT signal by actively clearing 5-HT from the extracellular space. Changes in SERT expression due to a common polymorphism in the promoter region has been linked to increased rates of depression after early life stress.[7–10] This transporter is also a prominent therapeutic target for many of the 5-HT-related disorders.[5] The most commonly used class of antidepressants, selective serotonin reuptake inhibitors (SSRIs, e.g. imipramine, citalopram, and paroxetine) selectively inhibit SERT to increase 5-HT levels.[11] There is evidence that the link between 5-HT and depression could be through serotonin-mediated potentiation of excitatory synapses in the CA1 region of the hippocampus,[12] although this remains an area of active investigation and controversy. Development of novel tools that can

help elucidate the complexities of 5-HT neurotransmission is crucial to understanding the role of this neurotransmitter in depression and other disorders.

Multiple techniques have been developed to measure changes in extracellular 5-HT levels, including microdialysis[13] and electrochemical[14,15] methods. Although these techniques are powerful and complementary (i.e., excellent chemical specificity of microdialysis/HPLC and high temporal resolution of electrochemical methods), they measure 5-HT release from potentially hundreds of synapses.[16]

In contrast, fluorescence microscopy provides both the spatial and temporal resolution to study rapid physiological events at the level of individual synapses. With respect to the serotonergic system, transgenic mouse lines (e.g., SERT-Cre, Pet1-Cre[17]) have been engineered to enable *in vivo* visualization of 5-HT neurons[18] and aspects of their activity when combined with genetically encoded tools, such as calcium sensors (GCaMPs).[19–21] However, there are no genetic tools to study 5-HT uptake through SERT, packaging into synaptic or secretory vesicles through the vesicular monoamine transporter (VMAT2), or release through exocytosis. Tracing 5-HT neurotransmission at the resolution of individual synapses has been achieved using small molecule probes, or even 5-HT itself, but each approach has limitations. Using three-photon microscopy, it is possible to directly image 5-HT fluorescence in the brain and study dynamic changes in its distribution,[22] but this method requires high laser power that can damage surrounding tissue, induces photobleaching, and has a low signal-to-noise ratio. Fluorescent SERT substrates have been developed based on the neurotoxin, MPP+ (4-phenyl-*N*-methylpyridinium),[23–25] including ASP+ (4-(4-dimethylaminostyryl)-*N*-methylpyridinium)[26–28] and APP+ (4-(4-dimethylamino)phenyl-1-methylpyridinium),[29,30] the latter of which is also a substrate for VMAT2. While these compounds offer some advantages over native 5-HT, particularly increased fluorescence, they also bind other intracellular organelles and are highly solvatochromic, which makes these probes poorly suited to measure the release of synaptic vesicle content from 5-HT neurons.[28,29] Additional prototypes of 5-HT fluorescent mimics have been reported, however without rigorous characterization at SERT.[31] These problems were resolved with 5,7-dihydroxytryptamine, a more fluorescent, pH-sensitive analog of 5-HT, which can be used to study vesicular packaging and release in 5-HT neurons via two-photon excitation with an improved signal-to-noise ratio.[32] Use of this compound is limited, however, due to high toxicity and the requirement of co-incubation with monoamine oxidation inhibitors.[32] Thus, there is a need for a non-toxic optical tracer of 5-HT that is widely applicable without requiring genetic manipulation or co-incubation with pharmacologically active agents.

Here we describe two fluorescent probes with improved properties for studying the 5-HT system, founded on the concept of fluorescent false neurotransmitters (FFNs) introduced by our group[33–35] (Figure 1A). Through optimization of the acridone core, we now identify FFN54 and FFN246 (Figure 1B) as fluorescent substrates of both SERT and VMAT2, and demonstrate the applicability of FFN246 for labeling serotonergic neurons in mouse brain tissue through SERT-dependent accumulation, while also highlighting features that require further improvement.

RESULTS and DISCUSSION

Design of Fluorescent SERT Substrates – FFN54 and Related Acridone Analogs

Development of new fluorophores or new versions of fluorophores with improved photophysical properties is an important endeavor.[36] In our laboratories, we have been focusing on designing optical substrates for enzymes and transporters by incorporating key recognition elements of relevant substrates into the fluorophore core.[37,38] For monoamine neurotransmitters, this was achieved by combining the arylethylamine fragment with the fluorescent coumarin core, thus identifying a series of VMAT2 substrates and dual dopamine transporter (DAT) and VMAT2 substrates that load and resolve individual dopaminergic synapses in mouse brain. These include, for example, compounds FFN200[35] and the pH-sensitive variant FFN102,[37,39] which revealed high levels of functional heterogeneity of dopaminergic synapses in mammalian striatum.

In designing a similar tool for the serotonergic system, however, none of the coumarin-based fluorophores we synthesized demonstrated significant substrate activity at SERT in cell-based uptake assays. We therefore examined a wide range of fluorophore cores integrated with the arylethylamine fragment, and identified FFN54, an acridone functionalized with the ethylamine on the 2-position (Figure 1). FFN54 showed hSERT-dependent cell uptake in a multi-well fluorometric assay using hSERT-transfected human kidney cells (hSERT-HEK, Figure 2). Cells were grown in 96-well plates and incubated with the experimental compounds (5 μM, 30 min) in the absence and presence of SERT inhibition (2 μM imipramine). Specific transporter uptake was determined by comparing the fluorescence intensity between the uninhibited wells (S for signal, which includes transporter-dependent and nonspecific uptake) and the inhibited wells (B for background, which only represents non-specific uptake), and expressed as a signal-to-basal ratio (S/B).

The structure activity relationship (SAR) between the acridone substitutions and SERT uptake was explored based on the following qualitative design considerations (Figure 2). The regio-isomers of FFN54 with the aminoethyl recognition group at different positions on the A-ring were synthesized (compounds **1**, **2**, and **3**) to vary the overall shape of the molecules and the relative configuration of the hydrogen bonding donors and acceptors, which we expect to cause marked differences in SERT transport parameters. Next, since the aminoethyl group serves as the key recognition element for the monoamine transporters,[40] the effects of both the length of the ethylene unit and the alkylation of the terminal amine were examined by preparing FFN54 analogs with one-methylene shorter and longer amino-alkyl side chains (compounds **4** and **5**), and mono- and di-methylamino groups (compounds **6** and **7**). We found that positional isomerism and/or other alterations of the aminoethyl group led to total loss of SERT activity (Figure 2B). With the basic molecular architecture defined, we next explored the steric and electronic effects (on both the transport and photophysical properties) by systematic substitution of the C-ring with a fluorine atom. The C-ring was chosen based on synthetic accessibility, and the fluorine atom owing to its small size and unique electronic properties. For example, placing the fluoro substituent in the 8-position (compound FFN246) or the 5-position (compound **10**, Figure 2A) was expected to have a strong effect on the hydrogen-bonding ability of the carbonyl and amine groups of the

acridone, as well as on the dipole moment of the entire molecule, which in turn would likely affect the interactions with the protein target and lower the background labeling. Importantly, the fluorine substitution scan of the C-ring identified the new lead of the acridone series, probe FFN246, which exhibits an improved S/B parameter (Figure 2B). The other fluoro-derivatives were completely inactive at SERT, demonstrating the dramatic effects of the fluorine substituent. Encouraged by the boost in activity of the 8-fluoro analog (**FFN246**), we explore this position further with both electron donating (CH_3) and electron withdrawing (Cl, CF_3) substituents (compounds **11**-**13**); however, increasing size of the group decreased the SERT activity of these 8-series analogs (compounds **13**-**15**). In summary, this systematic study provided a preliminary SAR map of the acridone system and identified FFN246 as a new lead.

With a new lead in hand, we determined FFN246's K_M constant at hSERT (14.3 ± 1.9 μM, Sup. Fig. S1C) using a modified initial rates assay.[41] We also examined the potential source of FFN246's improved performance using epifluorescence microscopy to visually compare cellular uptake and labeling morphology of uninhibited and inhibited (2 μM imipramine) hSERT-HEK cells. For both FFN54 and FFN246 probes, we observed a relatively diffuse intracellular fluorescent signal throughout the cell bodies (Figure 3A, D). Similar to the results of the fluorometric assay, we observed no difference in the intracellular fluorescence of FFN54 and FFN246 in the absence of inhibitor, but with increased contrast to detect low-level signal, it was apparent that there was substantially less background labeling with FFN246 than FFN54 in the presence of SERT inhibition (Figure 3C, F). Decreased non-specific uptake becomes highly important when applying these tools to *ex* and *in vivo* tissue, where the experimental systems are less uniform, and achieving an acceptable S/B in the neurons of interest is more challenging. Thus, the 110% increase of FFN246 specific uptake at hSERT (S/B = 6.5) over that of FFN54 (S/B = 3.0) can be attributed primarily to significantly lower non-specific uptake (B) while maintaining similar total signal (S, Figure 3G). This is likely explained by the difference in lipophilicity between FFN246 ($\log D_{oct/PBS}$ = 0.055) and FFN54 ($\log D_{oct/PBS}$ = 0.162), where FFN54 has a higher propensity to reside in hydrophobic compartments than FFN246. FFN246 is still relatively lipophilic compared to other FFNs, such as FFN102 (−1.45)[39] or FFN200 (−1.3),[35] which is relevant for the interpretation of the results in brain tissue (see below).

In terms of the photophysical properties, the fluoro substituent had a negligible effect, as both compounds share similar excitation and emission spectra (FFN54 ex/em (nm): 390/422; FFN246 ex/em (nm): 392/427) in an aqueous solvent, containing an emission band with two local maxima that is characteristic of acridone derivatives (Sup. Fig. S1B).[42,43]

Acridones FFN54 and FFN246 are Substrates of the Human Plasma Membrane Monoamine Transporters

To compare the uptake of FFN54 and FFN246 at other plasma membrane monoamine transporters, we used our multi-well fluorometric assay to measure SERT-, DAT-, and norepinephrine transporter (NET) dependent uptake in HEK cells stably transfected with human SERT (hSERT-HEK), NET (hNET-HEK), and DAT (hDAT-EM4), respectively. As described above, the specific uptake of experimental compounds (5 μM, 30 min) was

determined by comparing the fluorescence intensity between the uninhibited and inhibited wells (2 μM nomifensine for NET and DAT, 2 μM imipramine for SERT), and expressed as a signal-to-basal ratio (S/B) (Figure 3H).

FFN54 was the first compound to demonstrate SERT-dependent cellular uptake, but was not selective, as it showed uptake via all three transporters with similar signal-to-basal ratios (S/B = 2.7 to 3.1). With a single chemical modification, FFN246 showed significantly higher S/B ratios at all three transporters compared to FFN54, and demonstrated improved uptake at SERT relative to NET (23% lower) and DAT (31% lower, Figure 3H). This is a measurable improvement over the lead compound, FFN54, which demonstrated no significant difference in uptake between the three monoamine transporters (Figure 3H).

Examination of FFN246 Substrate Activity in VMAT2

To measure vesicular uptake and activity-dependent exocytosis in monoaminergic synapses, FFNs must also be substrates of VMAT2, the transporter responsible for synaptic and secretory vesicle loading of monoamine neurotransmitters in the central nervous system. VMAT2-dependent transport was measured using HEK cells stably transfected with rat VMAT2 (rVMAT2-HEK). In this cell line, VMAT2 actively transports substrates into acidic intracellular organelles[38,41,44] (Figure 4A). Therefore, using wide-field epifluorescence microscopy, VMAT2-dependent transport can be measured by imaging the intracellular distribution of the fluorescent compounds. In comparison to the hSERT-transfected HEK cells, these cells do not over-express the transporter on the plasma membrane, and as a result, a higher concentration of the probe (20 μM) was used to facilitate SERT-independent mechanisms for crossing the membrane (passive diffusion/equilibrative transporters).

rVMAT2-HEK cells treated with FFN246 showed a bright punctate fluorescence label consistent with accumulation of the compound in acidic organelles expressing VMAT2 (Figure 4D). The VMAT2-dependent accumulation was quantified and expressed as normalized total puncta fluorescence (number of puncta multiplied by average puncta fluorescence intensity then normalized to cellular coverage, Figure 4C). In contrast, when cells were pretreated with the VMAT inhibitors dihydrotetrabenazine (DTBZ, 2 μM) or reserpine (2 μM), this pattern was significantly reduced in both frequency and brightness (Figure 4E-F). The same was seen in null-transfected HEK cells (tetR-HEK, Figure 4G). These results suggest that VMAT-dependent vesicular loading of this compound in neurons is possible.

Since FFN246 exhibited substrate activity at SERT and VMAT2, it has potential as a 5-HT FFN. While it is not completely selective for SERT over DAT and NET, we further examined its properties and potential applications to study 5-HT neurons in more physiologically relevant experimental systems.

FFN246 Labels 5-HT Neuronal Soma in Mouse Brain.

To determine whether FFN246 is suitable for labeling neurons in endogenous systems, we first applied the probe (20 μM for 45 min) to the dorsal raphe (DR) region of acute mouse brain slices (Figure 5A), the primary region of 5-HT neuronal cell bodies in the brain. For this experiment, we crossed a reporter mouse line conditionally expressing eYFP linked to

channelrhodopsin-2[45] with a Cre-driver mouse line expressing Cre-recombinase under the *pet1* promoter[17]. The resulting bi-allelic mice carry the eYFP label in membranes of 5-HT neurons in developing and adult mice.[46] We observed FFN246 signal in 75% of 5-HT (eYFP-positive) neurons (81/108 total cells, 2–3 slices per animal, 3 different animals, Figure 5B-D). Pretreatment of the slices with an SSRI (2 μM imipramine or 200 nM citalopram) completely eliminated FFN246 uptake into 5-HT neurons, resulting in 0% of eYFP-positive neurons containing FFN246 signal (0/49 for imipramine, Figure 5, or 0/19 for citalopram, Sup. Fig. S2, 2–3 slices per animal, 2–3 different animals). The results indicate that FFN246 can be used to label 5-HT neurons in living tissue, and that accumulation into these cells is dependent on SERT activity. We also observed a small percentage of FFN246 labeled cells (7.4%) that did not express eYFP, as well as a relatively high background fluorescent signal that persisted through SERT inhibition, suggesting there is significant SERT-independent background uptake in brain tissue. We attempted to limit background uptake by repeating FFN246 uptake in 5-HT neurons in the presence of nomifensine (2 μM) to block any DAT/NET, but did not observe a significant change (Sup. Fig. S2). Perfusing a lower concentration of FFN246 (2 μM) over the tissue for a longer incubation time (60 min) also did not improve S/B (Sup. Fig. S3). These observations suggest that the relatively high lipophilic nature of the probe ($\log D_{oct/PBS} = 0.0545$) or transport by other transporters is responsible for the background signal.

Next, we examined whether FFN246 labels axonal projections from these 5-HT cell bodies. Since projections extend to various areas of the brain, we performed these experiments in multiple brain regions. Upon testing FFN246 uptake within the ventral striatum (Figure 6A-D) and the thalamus (Figure 6E-H), we did not observe any FFN246-labeled structures (> 2 SDs above background) that colocalized with 5-HT projections labeled by eYFP. SERT-specific uptake from these projections was not detectable above off-target uptake. However, when repeating this experiment in the substantia nigra reticulata (SNr, Figure 6I), which has more dense SERT expression,[47] we observed some FFN246 puncta that colocalized with axonal eYFP (Figure 6J-L), suggesting SERT-dependent labeling of 5-HT axonal varicosities. As observed in 5-HT cell bodies, pretreatment with an SSRI completely abolished any YFP and FFN colocalization (Sup. Fig. S4). However, the high level of background signal prevents wider applicability of FFN246 for 5-HT axonal labeling and functional studies as we have accomplished with DA FFNs.[35,39] Nevertheless, the latter results are encouraging and suggest the future directions for further development of the 5-HT FFN probes. As discussed in the design section above, FFN246 is still relatively lipophilic compared to DA FFNs,[35,39] which likely represents a major factor underlying the high background signal. This mechanistic (structure-property) insight will guide our future efforts aimed at developing improved 5-HT FFN probes.

Conclusions

SSRIs are widely used therapeutics targeting CNS disorders, and the third most common prescription drugs used by Americans.[48] The mechanisms by which SERT blockade exerts its therapeutic effects in depression and anxiety remain controversial,[49] highlighting the need for an improved understanding of the serotonergic system in the brain. Here, we describe the development of a novel fluorescent probe to study SERT activity in model cell

culture assays, 96-well screening assays, and *ex vivo* living brain tissue, without requiring genetic manipulation or co-incubation with other pharmacological agents. As an example, we demonstrated the use of FFN246 to readily measure the K_i's of both SSRIs used throughout these experiments (imipramine K_i = 4.8 ± 1.1 nM, and citalopram K_i = 1.6 ± 0.4 nM, Sup. Fig. S1D). FFN246 may also provide a means for directly examining SERT activity (and SERT ligands) in other cell preparations.[50] However, further improvement of the S/B ratio of labeled 5-HT structures in living tissue, as well as increasing selectivity between the plasma membrane monoamine transporters, remain important hurdles for developing a useful 5-HT FFN capable of illuminating the synaptic activity of the serotonergic system in the brain.

METHODS

Photophysical Characterization

Emission/Excitation—Excitation/Emission spectra were measured for each probe in Phosphate-buffered saline (PBS) buffer at a final concentration of 2 μM using a BioTek H1MF plate reader on bottom read mode.

Measurement of log D Values—The log *D* values were determined using the shake flask method in duplicate. First, 20 μM probe solution in 1 mL PBS was prepared, and then thoroughly mixed with 1 mL of *n*-octanol. This mixture was kept in dark for 3 days and allowed to reach equilibrium. The concentrations of probe in each layer were determined based on the UV absorbance. Log*D* values were determined based on the following equation; $\text{Log}D = \log[\text{probe}]_{\text{oct}} - \log[\text{probe}]_{\text{PBS}}$, in which $[\text{probe}]_{\text{oct}}$ and $[\text{probe}]_{\text{PBS}}$ are the concentrations of the probe in *n*-octanol and PBS, respectively.

FFN Characterization in Transfected Cell Culture

Cell culture preparation—For hNET and hSERT experiments, HEK293 cells stably transfected with hNET or hSERT were maintained in Dulbecco's Minimal Essential Medium (DMEM) with GlutaMAX (Invitrogen) supplemented with 10% (v/v) fetal bovine serum (FBS, Atlantis Biologicals), 500 μg/mL G418 (Calbiochem) to maintain the transgene, 100 U/mL Penicillin, and 10 μg/mL Streptomycin (Invitrogen). The hDAT-EM4 and HEK293 cells were maintained in the same culture medium without G418, and otherwise treated identically. For VMAT2 experiments, a HEK GNTI$^-$ (nonglycosylating) cell line stably expressing rVMAT2 (VMAT2-HEK) and a HEK GNTI$^-$ cell line stably transfected with TetR (TetR-HEK) to serve as a control were provided by the lab of Professor Robert Edwards (UCSF), and have been described in detail.[44] These were maintained as previously reported by our labs.[38,41] All cells were routinely cultured in 10 cm polystyrene culture plates (Falcon), were subcultured before reaching confluence (every 3–4 days), and were maintained in a humidified atmosphere at 37 °C containing 5% CO_2. On the day of experiments, the growth medium was replaced by experimental medium (DMEM minus phenol red with 4 mM L-glutamine (Invitrogen), 1 % (v/v) FBS (Atlanta Biologicals), 100 U/mL penicillin (Invitrogen) and 100 μg/mL streptomycin (Invitrogen)) with and without inhibitors as described below.

Evaluation of hNET, hDAT, and hSERT substrate activity via fluorometric assay—Stably transfected hNET-HEK, hDAT-HEK, and hSERT-HEK cells were seeded at a density of 0.08–0.09 × 10^6 cells/well in white solid-bottom 96-well plates and allowed to proliferate in growth medium for ~2 days at 37 °C to reach confluence. At the start of the experiment, the growth medium was aspirated, wells were washed with 200 μL PBS, and then treated with 100 μL experimental medium with DMSO (vehicle, 0.02% v/v) or inhibitor (2 μM nomifensine for hNET-HEK and hDAT-EM4 cells, 2 μM imipramine for hSERT-HEK cells). The cells were incubated for 60 min at 37 °C, and then experimental compounds (5 μM) were added. After probe incubation for 30 min at 37 °C the experiment was terminated by three rapid PBS washes. The fluorescence uptake in cells was immediately recorded using a BioTek H1MF plate reader with excitation and emission wavelengths set at 389 nm and 442 nm respectively. Substrate activity was determined using signal to basal ratio (S/B): mean fluorescence uptake of the probe (with DMSO vehicle) divided by that in the presence of inhibitor (nomifensine or imipramine). Data presented as normalized uptake ± SEM from six independent plates across three days (four separate measurements per plate). Significance was determined using a one-way ANOVA with Dunnett's Multiple Comparison Test.

Determination of FFN246's K_M in hSERT-HEK cells[41]—Stably transfected hSERT-HEK cells were prepared in 96-well plates as described above. To determine the linear region of uptake, growth medium was aspirated, cells were washed with 200 μL PBS, treated with 20 μM FFN246 in experimental medium at room temperature for a series of time points, washed twice with 200 μL PBS, replaced with 120 μL PBS, and then fluorescence was read using the plate reader. Treatment time ranged from 3 to 18 min at 3 min intervals. Since uptake was linear at this range, 10-min treatment time was used for the K_M determination. For the K_M determination, wells were washed with 200 μL, treated with 100 μL experimental medium with DMSO or 2 μM imipramine, and incubated for 60 min at 37 °C. The medium was then aspirated, and wells were replaced with the same experimental medium (with DMSO or imipramine), mixed well with FFN246 of varying concentrations (1 to 50 μM). Cells were incubated at room temperature for 10 min, then washed twice with 200 μL PBS, then in 120 μL PBS fluorescence was read using the plate reader.

Determination of K_i Values for Known SSRIs, Imipramine and Citalopram, at Serotonin Transporter in Cellular Cultures Using FFN246 as Substrate—Stably transfected hSERT-HEK cells were prepared in 96-well plates as described above. At the onset of the experiment, the growth medium of confluent cells was aspired and then cells were pre-incubated with 63 μL of experimental media solutions containing a different concentration of an inhibitor (imipramine or citalopram) or DMSO vehicle for 1 hour. 63 μL of experimental media containing FFN246 was then added (final FFN concentration: 2.5 μM) and incubated for 30 min. The plates were then washed with 120 μL of PBS. The fluorescence uptake in each well of the plate was immediately recorded on the BioTek H1MF plate reader. The specific uptake was defined as described above, and analyzed using Dose-Response – Inhibitor nonlinear regression analysis ([Inhibitor] vs. Response (three parameters)) as provided by the GraphPad Prism 6 software to quantify the respective IC_{50} value ± SEM for each inhibitor. The determination of the K_i value ± SEM for each inhibitor

is calculated using the Cheng-Prusoff equation,[52] with the following established parameters: K_M (for FFN246) = 14 μM and the concentration of FFN246 in this experiment (2.5 μM).

Fluorescence microscopy imaging of probes in hSERT-HEK cells—hSERT-HEK and control HEK293 cells were plated onto poly-D-lysine (Sigma Aldrich, c = 0.1 mg/mL) coated clear bottom six-well plates at a density of 0.15–0.20 × 10^6 cells per well and grown at 37°C in 5% CO_2 (v/v). After 4 days of growth, the cells reached 80–90% confluence and then the culture medium was removed by aspiration, and the cells were washed with PBS. Cells were then incubated in 0.9 mL of experimental media containing the imipramine (2 μM) or DMSO vehicle as a control at 37°C in 5% CO_2 for 1 h. The compound uptake was initiated by adding 0.1 mL of experimental media containing probe (final probe concentration of 20 μM) with and without imipramine (2 μM). Following incubation at 37° C in 5% CO_2 for 30 min, the media was removed by aspiration and the cells were washed with PBS and maintained in fresh experimental media. Fluorescence images (at least 3 images/well in duplicate wells) were acquired with a Leica FW 4000 imaging system (Leica Microsystems) equipped with a Chroma custom filter cube (λ_{ex} = 350 ± 25 nm, λ_{em} = 460 ± 25 nm; Chroma Technology Corporation) and a Leica DFC-360FX camera. Fluorescence and bright field images were acquired with exposure time set at 600 ms and 37 ms respectively. All images were adjusted using the same contrast and brightness level using ImageJ software (National Institutes of Health).

Fluorescence microscopy imaging of probes in rVMAT2-HEK cells—Epifluorescence microscopy as reported here was conducted as previously reported using rVMAT2-HEK and control TetR-HEK cells.[41] Briefly, VMAT-HEK and TetR-HEK cells were plated at a density of 0.15–0.20 × 10^6 cells per well on poly-D-lysine coated 6-well optical plates (Falcon) and grown at 37 °C in 5% CO_2 (v/v). Following ~4 days of growth, the cells had reached 80–90% confluence. The culture medium was removed by aspiration, the cells were washed with PBS (Invitrogen, 1.0 mL/well), and the wells were pretreated with experimental medium with or without the VMAT2 inhibitors reserpine (2 μM, Sigma-Aldrich) or dihydrotetrabenazine (DTBZ, 2 μM; Sigma-Aldrich) for 60 min. To initiate uptake, solutions of experimental probe with or without inhibitor were added to the appropriate wells for a final concentration of 20 μM probe with or without reserpine (2 μM) or DTBZ (2 μM). Cells were incubated at 37°C for 1 h, at which point the probe solutions were removed by aspiration and wells were gently washed with PBS (2 mL). Wells were maintained in fresh experimental medium and were imaged as described above.

Quantification of VMAT2 substrate activity—The Multiple Thresholds ImageJ plug-in (created by Damon Poburko, Simon Fraser University, Burnaby, BC, Canada) was used for quantification of fluorescent puncta in images of rVMAT2-HEK cells obtained from fluorescence microscopy. Puncta were identified as objects conforming to defined parameters: brightness (> 0.6 SDs above background), appropriate size (0.5 – 4 μm^2), rounded shape (min circularity: 0.6), and well delimited boundaries. Data presented as mean intensity of these puncta structures per image, normalized to cellular coverage of the field of view (as measured by area of fluorescent signal 2 SDs above background) ± SEM from four

independent experiments (six images per condition per experiment). Significance was determined using a one-way ANOVA with Dunnett's Multiple Comparison Test.

Determination of FFN Loading in Acute Murine Brain Slices

Acute murine brain slice preparation—All animals used for slice preparation were Cg-Tg(Fev-cre)1Esd/J (ePet-cre, Jackson Laboratory) crossed with Ai32(RCL-ChR2(H134R)/EYFP (Ai32, Jackson Laboratory) maintained on a 129SvEv/Tac background. Double transgenic animals were housed in a 12h light/dark cycle with access to food and water ad libitum. Animals were sacrificed at the age of 9–11 weeks. All animal protocols were approved by the IACUC of Columbia University. Mice were decapitated and acute 300 μm thick coronal slices were cut on a Leica VT1200 vibratome (Leica Microsystems) at 4 °C and then allowed to recover for 1 h in oxygenated (95% O_2, 5% CO_2) artificial cerebrospinal fluid (ACSF) containing (in mM): 125 NaCl, 2.5 KCl, 26 $NaHCO_3$, 0.3 KH_2PO_4, 2.4 $CaCl_2$, 1.3 $MgSO_4$, 0.8 NaH_2PO_4, 10 Glucose (pH = 7.2–7.4, 292–296 mOsm/L). Slices were then used at room temperature for all imaging experiments.

Application and 2-photon imaging of FFN246—Slices were incubated with FFN246 (20 μM) for 30 min and then transferred to an imaging chamber (QE-1, Warner Instruments, Hamden, CT) and held in place by a platinum wire and nylon string custom made holder and superfused (1 mL/min) with oxygenated ACSF.[53] Slices were washed in the perfusion chamber for 10 min before imaging. For inhibition experiments, slices were first pre-incubated with imipramine (2 μM) for 15 min, and then co-incubated with the FFN for the 30 min loading period. Inhibitor was also added to the perfusing ACSF solution. Fluorescent structures were visualized at depths of at least 25 μm from the slice surface using a Prairie Ultima Multiphoton Microscopy System (Prairie Technologies, Middleton, WI) with a titanium-sapphire Chameleon Ultra II laser (Coherent, Santa Clara, CA) equipped with a 60 X 0.9 NA water immersion objective. FFN246 was excited at 760 nm and 435–485 nm light was collected. eYFP was excited at 950 nm and 500–550 nm light was collected. Images were captured in 16-bit 112 × 112 μm^2 field of view at 512 × 512 $pixel^2$ resolution and a dwell time of 10 μs/pixel using Prairie View software.

Uptake of FFN246 within eYFP-positive 5-HT cells—5-HT neurons were identified in the dorsal raphe nucleus if they had visually continuous coronal eYFP fluorescence that was greater than two standard deviations above background. The number of 5-HT cells that also loaded FFN246 was determined by measuring the percentage of 5-HT cells that also contained FFN fluorescence greater than two standard deviations above background. For potential colocalization of FFN246 and 5-HT axonal projections, brain slices were collected which contained the ventral striatum or thalamus or the substantia nigra reticulata. In all regions, we observed detectable eYFP signal, but colocalizing FFN246 signal (two standard deviations above background levels) was only in the SNr.

Supplementary Material

Refer to Web version on PubMed Central for supplementary material.

ACKNOWLEDGMENT

This work was supported by the G. Harold & Y. Mathers Charitable Foundation (D. Sames), National Institutes of Health (R01MH086545 to D. Sames, R01MH108186 to D. Sames and D. Sulzer, R01DA07418 to D. Sulzer, and R00MH083044 to M.S. Ansorge), the Sackler Institute for Developmental Psychobiology (M.S. Ansorge), the FWF graduate program (Molecular Drug Targets W 1232 to D. Dreier), and the JPB Foundation (D. Sulzer). D. Sulzer is a Brain and Behavior Research Foundation Distinguished Investigator.

ABBREVIATIONS

5-HT	serotonin, 5-hydroxytryptamine
DAT	dopamine transporter
DR	dorsal raphe nucleus
DTBZ	dihydrotetrabenazine
FFN	fluorescent false neurotransmitter
NET	norepinephrine transporter
SERT	serotonin transporter
SNr	substantia nigra reticulata
VMAT2	vesicular monoamine transporter 2

REFERENCES

(1). Jacobs BL, and Azmitia EC (1992) Structure and function of the brain serotonin system. *Physiol.* Rev. 72, 165–229. [PubMed: 1731370]

(2). Roth BL, Hanizavareh SM, and Blum AE (2004) Serotonin receptors represent highly favorable molecular targets for cognitive enhancement in schizophrenia and other disorders. Psychopharmacology (Berl). 174, 17–24. [PubMed: 15205874]

(3). Berger M, Gray JA, and Roth BL (2009) The expanded biology of serotonin. *Annu. Rev. Med.* 60, 355–66. [PubMed: 19630576]

(4). Gershon MD, and Tack J (2007) The serotonin signaling system: from basic understanding to drug development for functional GI disorders. Gastroenterology 132, 397–414. [PubMed: 17241888]

(5). Ni W, and Watts SW (2006) 5-hydroxytryptamine in the cardiovascular system: focus on the serotonin transporter (SERT). *Clin. Exp. Pharmacol.* Physiol. 33, 575–83. [PubMed: 16789923]

(6). Frick A, Åhs F, Engman J, Jonasson M, Alaie I, Björkstrand J, Frans Ö, Faria V, Linnman C, Appel L, Wahlstedt K, Lubberink M, Fredrikson M, and Furmark T (2015) Serotonin Synthesis and Reuptake in Social Anxiety Disorder: A Positron Emission Tomography Study. JAMA psychiatry 72, 794–802. [PubMed: 26083190]

(7). Nutt DJ (2002) The neuropharmacology of serotonin and noradrenaline in depression. *Int. Clin.* Psychopharmacol. 17 Suppl 1, S1–12.

(8). Arango V, Underwood MD, Boldrini M, Tamir H, Kassir SA, Hsiung S, Chen JJ, and Mann JJ (2001) Serotonin 1A Receptors, Serotonin Transporter Binding and Serotonin Transporter mRNA Expression in the Brainstem of Depressed Suicide Victims. Neuropsychopharmacology 25, 892–903. [PubMed: 11750182]

(9). Bradley CC, and Blakely RD (1997) Alternative splicing of the human serotonin transporter gene. *J. Neurochem.* 69, 1356–67. [PubMed: 9326263]

(10). Vergne DE, and Nemeroff CB (2006) The interaction of serotonin transporter gene polymorphisms and early adverse life events on vulnerability for major depression. *Curr. Psychiatry Rep.* 8, 452–7. [PubMed: 17094925]

(11). Nemeroff CB, and Owens MJ (2009) The role of serotonin in the pathophysiology of depression: as important as ever. *Clin.* Chem. 55, 1578–9. [PubMed: 19498050]

(12). Cai X, Kallarackal AJ, Kvarta MD, Goluskin S, Gaylor K, Bailey AM, Lee HK, Huganir RL, and Thompson SM (2013) Local potentiation of excitatory synapses by serotonin and its alteration in rodent models of depression. *Nat.* Neurosci. 16, 464–72. [PubMed: 23502536]

(13). Yang H, Sampson MM, Senturk D, and Andrews AM (2015) Sex- and SERT-Mediated Differences in Stimulated Serotonin Revealed by Fast Microdialysis. ACS Chem. Neurosci 6, 1487–1501. [PubMed: 26167657]

(14). Hashemi P, Dankoski EC, Wood KM, Ambrose RE, and Wightman RM (2011) In vivo electrochemical evidence for simultaneous 5-HT and histamine release in the rat substantia nigra pars reticulata following medial forebrain bundle stimulation. *J.* Neurochem. 118, 749–59. [PubMed: 21682723]

(15). Hashemi P, Dankoski EC, Petrovic J, Keithley RB, and Wightman RM (2009) Voltammetric detection of 5-hydroxytryptamine release in the rat brain. *Anal. Chem.* 81, 9462–71. [PubMed: 19827792]

(16). Sames D, Dunn M, Karpowicz RJ, and Sulzer D (2013) Visualizing neurotransmitter secretion at individual synapses. *ACS Chem. Neuro*sci. 4, 648–51. [PubMed: 23862751]

(17). Scott MM, Wylie CJ, Lerch JK, Murphy R, Lobur K, Herlitze S, Jiang W, Conlon RA, Strowbridge BW, and Deneris ES (2005) A genetic approach to access serotonin neurons for in vivo and in vitro studies. *Proc. Natl. Acad. Sci. U. S.* A. 102, 16472–7. [PubMed: 16251278]

(18). Zhuang X, Masson J, Gingrich JA, Rayport S, and Hen R (2005) Targeted gene expression in dopamine and serotonin neurons of the mouse brain. J. Neurosci. Methods 143, 27–32. [PubMed: 15763133]

(19). Li Y, Zhong W, Wang D, Feng Q, Liu Z, Zhou J, Jia C, Hu F, Zeng J, Guo Q, Fu L, Luo M, Schultz W, Dayan P, Montague PR, Wise RA, Berridge KC, Cohen JY, Haesler S, Vong L, Lowell BB, Uchida N, Jacobs BL, Azmitia EC, Weissbourd B, Ogawa SK, Cohen JY, Hwang D, Uchida N, Watabe-Uchida M, Dorocic IP, Mann JJ, Vaswani M, Linda FK, Ramesh S, Luo M, Zhou J, Liu Z, Simansky KJ, Lucki I, Liu Y, Cools R, Nakamura K, Daw ND, Simon H, Le Moal, M., Cardo B, Liu Z, Qi J, McDevitt RA, Miyazaki K, Miyazaki KW, Doya K, Miyazaki KW, Madalena SF, Murakami M, Zachary FM, Zhou J, Jia C, Feng Q, Bao J, Luo M, Sakai K, Crochet S, Ranade SP, Mainen ZF, Li Y, Dalphin N, Hyland BI, Fornal CA, Metzler CW, Marrosu F, Ribiero-do-Valle LE, Jacobs BL, Waterhouse BD, Devilbiss D, Seiple S, Markowitz R, Nakamura K, Matsumoto M, Hikosaka O, Bromberg-Martin ES, Hikosaka O, Nakamura K, Hayashi K, Nakao K, Nakamura K, Inaba K, Schweimer JV, Ungless MA, Hioki H, Fu W, Calizo LH, Allers KA, Sharp T, Hajos M, Cohen JY, Amoroso MW, Uchida N, Challis C, Spoida K, Masseck OA, Deneris ES, Herlitze S, Amat J, Warden MR, Flusberg BA, Cui G, Gunaydin LA, Chen TW, Gong S, Zhang X, Beaulieu JM, Sotnikova TD, Gainetdinov RR, Caron MG, Bevins RA, Besheer J, Hintiryan H, Hayes UL, Chambers KC, Kvitsiani D, Anikeeva P, Luo M, Fee MS, Katz LC, Chao HT, Zhao S, Miyazaki KW, Miyazaki K, Doya K, Ranade S, Pi HJ, Kepecs A, Miyazaki K, Miyazaki KW, Doya K, Miyazaki KW, Miyazaki K, Doya K, Kocsis B, Varga V, Dahan L, Sik A, Jensen P, Liu C, Gras C, Shikanai H, Dayan P, Huys QJ, Boureau YL, Dayan P, Groppe DM, Urbach TP, and Kutas M (2016) Serotonin neurons in the dorsal raphe nucleus encode reward signals. *Nat. Commun.* 7, 10503. [PubMed: 26818705]

(20). Yu Q, Teixeira CM, Mahadevia D, Huang Y, Balsam D, Mann JJ, Gingrich JA, and Ansorge MS (2014) Dopamine and serotonin signaling during two sensitive developmental periods differentially impact adult aggressive and affective behaviors in mice. Mol. Psychiatry 19, 688–698. [PubMed: 24589889]

(21). Chen T-W, Wardill TJ, Sun Y, Pulver SR, Renninger SL, Baohan A, Schreiter ER, Kerr RA, Orger MB, Jayaraman V, Looger LL, Svoboda K, and Kim DS (2013) Ultrasensitive fluorescent proteins for imaging neuronal activity. Nature 499, 295–300. [PubMed: 23868258]

(22). Maiti S, Shear JB, Williams RM, Zipfel WR, and Webb WW (1997) Measuring serotonin distribution in live cells with three-photon excitation. Science 275, 530–2. [PubMed: 8999797]

(23). Javitch JA, D'Amato RJ, Strittmatter SM, and Snyder SH (1985) Parkinsonism-inducing neurotoxin, N-methyl-4-phenyl-1,2,3,6 -tetrahydropyridine: uptake of the metabolite N-methyl-4-phenylpyridine by dopamine neurons explains selective toxicity. *Proc. Natl. Acad.* Sci. 82, 2173–2177. [PubMed: 3872460]

(24). Wall SC, Gu H, and Rudnick G (1995) Biogenic amine flux mediated by cloned transporters stably expressed in cultured cell lines: amphetamine specificity for inhibition and efflux. *Mol.* Pharmacol. 47, 544–50. [PubMed: 7700252]

(25). Gainetdinov RR, Fumagalli F, Jones SR, and Caron MG (1997) Dopamine transporter is required for in vivo MPTP neurotoxicity: evidence from mice lacking the transporter. *J. Neurochem.* 69, 1322–5. [PubMed: 9282960]

(26). Oz M, Libby T, Kivell B, Jaligam V, Ramamoorthy S, and Shippenberg TS (2010) Real-time, spatially resolved analysis of serotonin transporter activity and regulation using the fluorescent substrate, ASP+. *J. Neurochem.* 114, 1019–1029. [PubMed: 20524964]

(27). Fowler A, Seifert N, Acker V, Woehrle T, Kilpert C, and de Saizieu A (2006) A nonradioactive high-throughput/high-content assay for measurement of the human serotonin reuptake transporter function in vitro. *J. Biomol. Screen.* 11, 1027–34. [PubMed: 17099247]

(28). Schwartz JW, Blakely RD, and DeFelice LJ (2003) Binding and transport in norepinephrine transporters. Real-time, spatially resolved analysis in single cells using a fluorescent substrate. *J. Biol.* Chem. 278, 9768–77. [PubMed: 12499385]

(29). Karpowicz RJ, Dunn M, Sulzer D, and Sames D (2013) APP+, a fluorescent analogue of the neurotoxin MPP+, is a marker of catecholamine neurons in brain tissue, but not a fluorescent false neurotransmitter. ACS Chem. Neurosci 4, 858–69. [PubMed: 23647019]

(30). Bernstein AI, Stout KA, and Miller GW (2012) A fluorescent-based assay for live cell, spatially resolved assessment of vesicular monoamine transporter 2-mediated neurotransmitter transport. J. Neurosci. Methods 209, 357–66. [PubMed: 22698664]

(31). Brown AS, Bernal L-M, Micotto TL, Smith EL, and Wilson JN (2011) Fluorescent neuroactive probes based on stilbazolium dyes. *Org. Biomol.* Chem. 9, 2142–8. [PubMed: 21293810]

(32). Colgan LA, Putzier I, and Levitan ES (2009) Activity-dependent vesicular monoamine transporter-mediated depletion of the nucleus supports somatic release by serotonin neurons. *J.* Neurosci. 29, 15878–87. [PubMed: 20016104]

(33). Gubernator NG, Zhang H, Staal RGW, Mosharov EV, Pereira DB, Yue M, Balsanek V, Vadola PA, Mukherjee B, Edwards RH, Sulzer D, and Sames D (2009) Fluorescent false neurotransmitters visualize dopamine release from individual presynaptic terminals. Science 324, 1441–4. [PubMed: 19423778]

(34). Zhang H, Gubernator NG, Yue M, Staal RGW, Mosharov EV, Pereira D, Balsanek V, Vadola PA, Mukherjee B, Edwards RH, Sulzer D, and Sames D (2009) Dopamine Release at Individual Presynaptic Terminals Visualized with FFNs. J. Vis. Exp e1562–e1562.

(35). Pereira DB, Schmitz Y, Mészáros J, Merchant P, Hu G, Li S, Henke A, Lizardi-Ortiz JE, Karpowicz RJ, Morgenstern TJ, Sonders MS, Kanter E, Rodriguez PC, Mosharov EV, Sames D, and Sulzer D (2016) Fluorescent false neurotransmitter reveals functionally silent dopamine vesicle clusters in the striatum. *Nat.* Neurosci. 19, 578–86. [PubMed: 26900925]

(36). Lavis LD (2017) Teaching Old Dyes New Tricks: Biological Probes Built from Fluoresceins and Rhodamines. *Annu. Rev. Biochem.* 86, 825–843. [PubMed: 28399656]

(37). Froemming MK, and Sames D (2007) Harnessing functional plasticity of enzymes: A fluorogenic probe for imaging 17β-HSD10 dehydrogenase, an enzyme involved in Alzheimer's and Parkinson's diseases. *J. Am. Chem.* Soc. 129, 14518–14522. [PubMed: 17958419]

(38). Lee M, Gubernator NG, Sulzer D, and Sames D (2010) Development of pH-responsive fluorescent false neurotransmitters. *J. Am. Chem.* Soc. 132, 8828–30. [PubMed: 20540519]

(39). Rodriguez PC, Pereira DB, Borgkvist A, Wong MY, Barnard C, Sonders MS, Zhang H, Sames D, and Sulzer D (2013) Fluorescent dopamine tracer resolves individual dopaminergic synapses and their activity in the brain. *Proc. Natl. Acad. Sci. U. S.* A. 110, 870–5. [PubMed: 23277566]

(40). Partilla JS, Dempsey AG, Nagpal AS, Blough BE, Baumann MH, and Rothman RB (2006) Interaction of Amphetamines and Related Compounds at the Vesicular Monoamine Transporter. *J.* Pharmacol. Exp. Ther. 319, 237–246. [PubMed: 16835371]

(41). Hu G, Henke A, Karpowicz RJ, Sonders MS, Farrimond F, Edwards R, Sulzer D, and Sames D (2013) New fluorescent substrate enables quantitative and high-throughput examination of vesicular monoamine transporter 2 (VMAT2). *ACS Chem.* Biol. 8, 1947–54. [PubMed: 23859623]

(42). Smith JA, and West RM (2011) Acridone derivatives as labels for fluorescence detection of target materials. U. S

(43). Brown RD, and Lahey FN (1949) The Ultraviolet Absorption Spectra of the Acridone Alkaloids. Aust. J. Sci. Res 3, 593.

(44). Adam Y, Edwards RH, and Schuldiner S (2008) Expression and function of the rat vesicular monoamine transporter 2. *Am. J. Physiol. Cell Physiol.* 294, C1004–11. [PubMed: 18287335]

(45). Madisen L, Mao T, Koch H, Zhuo J, Berenyi A, Fujisawa S, Hsu Y-WA, Garcia AJ, Gu X, Zanella S, Kidney J, Gu H, Mao Y, Hooks BM, Boyden ES, Buzsáki G, Ramirez JM, Jones AR, Svoboda K, Han X, Turner EE, and Zeng H (2012) A toolbox of Cre-dependent optogenetic transgenic mice for light-induced activation and silencing. *Nat.* Neurosci. 15, 793–802. [PubMed: 22446880]

(46). Pelosi B, Migliarini S, Pacini G, Pratelli M, and Pasqualetti M (2014) Generation of Pet1210-Cre transgenic mouse line reveals non-serotonergic expression domains of Pet1 both in CNS and periphery. PLoS One 9, e104318. [PubMed: 25098329]

(47). Perez XA, Bianco LE, and Andrews AM (2006) Filtration disrupts synaptosomes during radiochemical analysis of serotonin uptake: Comparison with chronoamperometry in SERT knockout mice. J. Neurosci. Methods 154, 245–255. [PubMed: 16472867]

(48). (2011) National Center for Health Statistics Health, United States, 2010: With Special Feature on Death and Dying. Hyattsville, MD Hyattsville, MD.

(49). Al-Harbi KS (2012) Treatment-resistant depression: therapeutic trends, challenges, and future directions. Patient Prefer. Adherence 6, 369–88. [PubMed: 22654508]

(50). Beikmann BS, Tomlinson ID, Rosenthal SJ, and Andrews AM (2013) Serotonin Uptake Is Largely Mediated by Platelets versus Lymphocytes in Peripheral Blood Cells. *ACS Chem.* Neurosci. 4, 161–170. [PubMed: 23336055]

(51). Lein ES, Hawrylycz MJ, Ao N, Ayres M, Bensinger A, Bernard A, Boe AF, Boguski MS, Brockway KS, Byrnes EJ, Chen L, Chen L, Chen T-M, Chi Chin M, Chong J, Crook BE, Czaplinska A, Dang CN, Datta S, Dee NR, Desaki AL, Desta T, Diep E, Dolbeare TA, Donelan MJ, Dong H-W, Dougherty JG, Duncan BJ, Ebbert AJ, Eichele G, Estin LK, Faber C, Facer BA, Fields R, Fischer SR, Fliss TP, Frensley C, Gates SN, Glattfelder KJ, Halverson KR, Hart MR, Hohmann JG, Howell MP, Jeung DP, Johnson RA, Karr PT, Kawal R, Kidney JM, Knapik RH, Kuan CL, Lake JH, Laramee AR, Larsen KD, Lau C, Lemon TA, Liang AJ, Liu Y, Luong LT, Michaels J, Morgan JJ, Morgan RJ, Mortrud MT, Mosqueda NF, Ng LL, Ng R, Orta GJ, Overly CC, Pak TH, Parry SE, Pathak SD, Pearson OC, Puchalski RB, Riley ZL, Rockett HR, Rowland SA, Royall JJ, Ruiz MJ, Sarno NR, Schaffnit K, Shapovalova NV, Sivisay T, Slaughterbeck CR, Smith SC, Smith KA, Smith BI, Sodt AJ, Stewart NN, Stumpf K-R, Sunkin SM, Sutram M, Tam A, Teemer CD, Thaller C, Thompson CL, Varnam LR, Visel A, Whitlock RM, Wohnoutka PE, Wolkey CK, Wong VY, Wood M, Yaylaoglu MB, Young RC, Youngstrom BL, Feng Yuan X, Zhang B, Zwingman TA, and Jones AR (2007) Genome-wide atlas of gene expression in the adult mouse brain. Nature 445, 168–176. [PubMed: 17151600]

(52). Yung-Chi C, and Prusoff WH (1973) Relationship between the inhibition constant (KI) and the concentration of inhibitor which causes 50 per cent inhibition (I50) of an enzymatic reaction. *Biochem.* Pharmacol. 22, 3099–3108. [PubMed: 4202581]

(53). Wong MY, Sulzer D, and Bamford NS (2011) Imaging presynaptic exocytosis in corticostriatal slices. *Methods Mol.* Biol. 793, 363–76. [PubMed: 21913113]

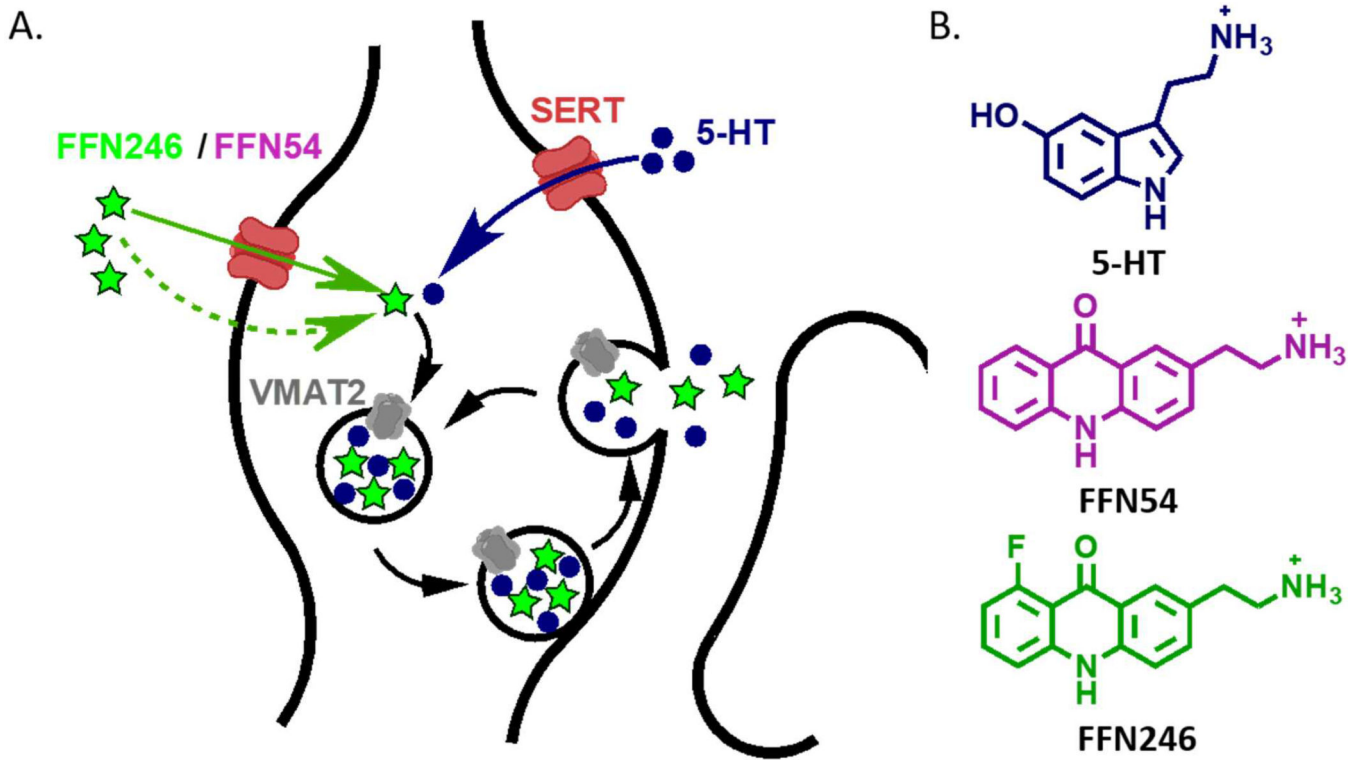

Figure 1.

The concept and design of serotoninergic fluorescent false neurotransmitters (5-HT FFNs). A) 5-HT FFN Concept: As a fluorescent tracer of the native 5-HT neurotransmitter, the 5-HT FFN is transported into the serotonergic presynaptic varicosities (shown here) or cell bodies through the plasma membrane serotonin transporter, SERT, followed by packaging into synaptic vesicles via the vesicular monoamine transporter, VMAT2. Upon stimulation, the vesicles undergo exocytosis and release 5-HT and potentially FFN into the extracellular space. B) 5-HT FFN Design: key structural features of the 5-HT neurotransmitter are fused into a fluorophore core. In addition to the SERT and VMAT2 transport, the compounds must be sufficiently bright, photostable, and biocompatible. From of a wide structural space of fluorophores examined, only acridones met all these criteria. We introduce two novel fluorescent compounds, FFN54 and FFN246 as dual substrates of SERT and VMAT2.

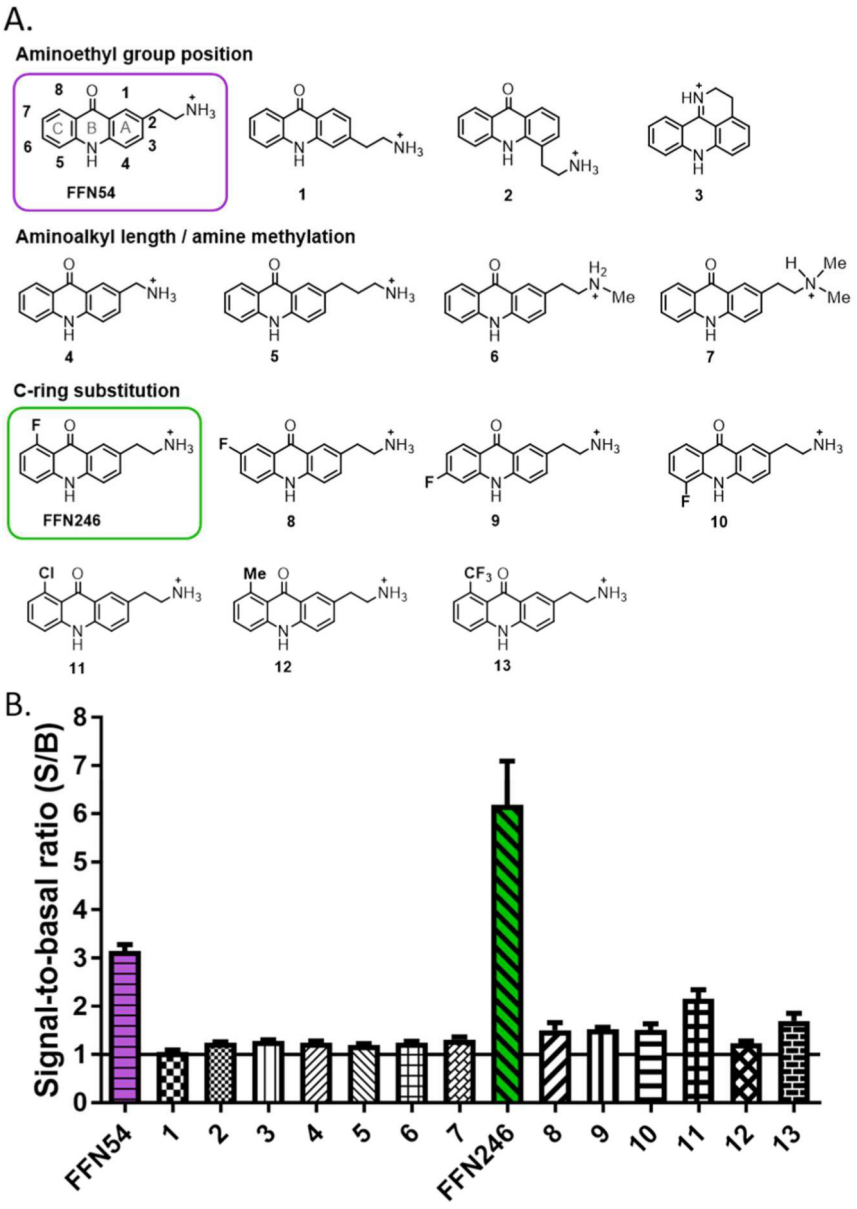

Figure 2.

Systematic structure-activity study identified acridone leads FFN54 and FFN246 demonstrate hSERT uptake. A) A focused library of acridone analogs examined the effect of position and nature of the aminoalkyl recognition element, as well as the C-ring substitution on hSERT uptake. B) Total cellular fluorescence of hSERT-transfected HEK cells after incubation with the compound (5μM, plate-reader assay). Signal-to-basal ratio (S/B) was determined by comparing cellular fluorescence in the presence (basal, B) and absence (signal, S) of inhibitor (2 μM imipramine) after a 30 min incubation period.

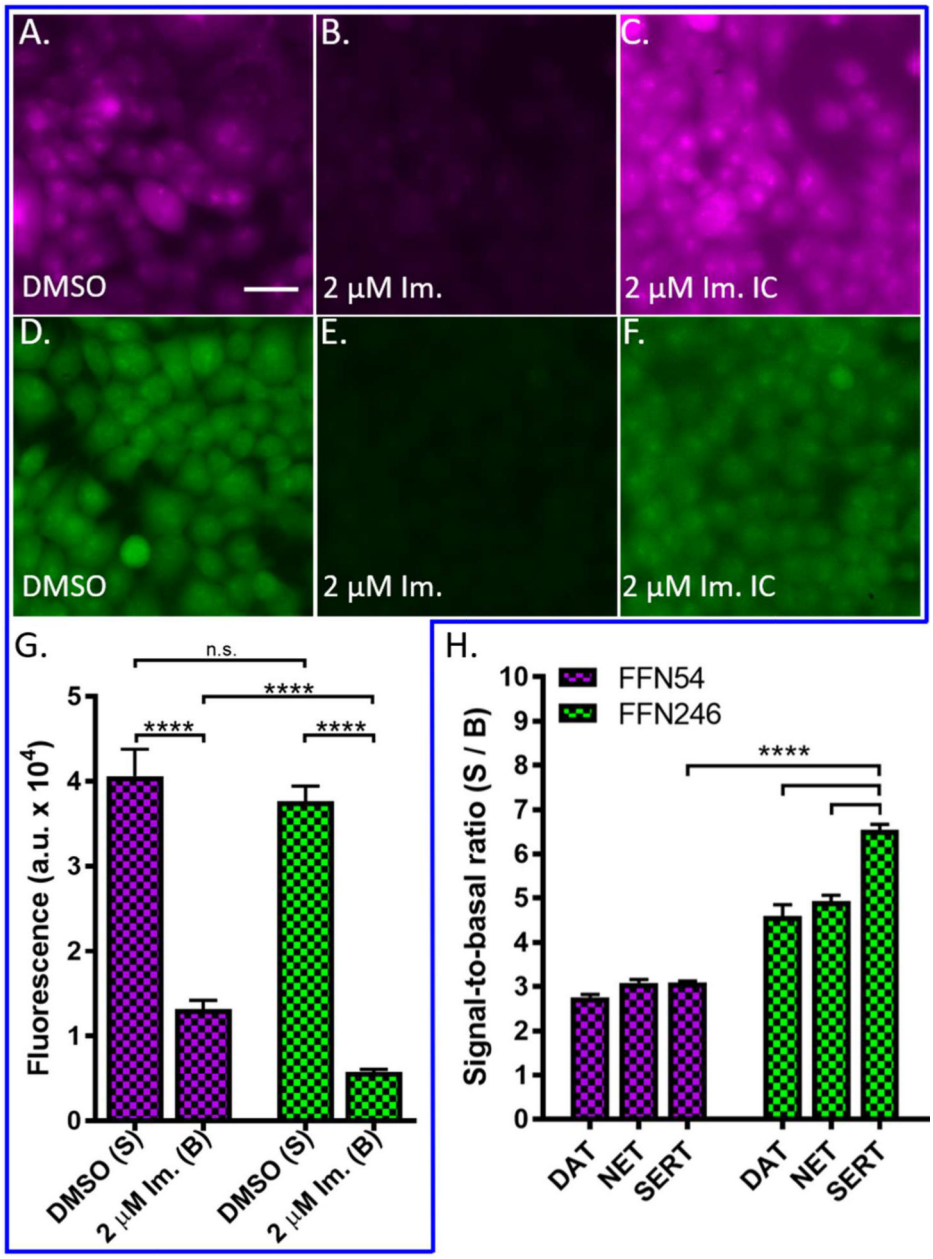

Figure 3.

Probes FFN54 and FFN246 display different levels of background labeling and transporter selectivity. G) Quantification of fluorescence uptake of FFN probes in HEK cells expressing hSERT in the presence and absence of 2 μM imipramine as measured by epifluorescence. Uninhibited cellular uptake of both FFN54 and FFN246 were comparable, reflected in representative images A and D, respectively. The signal of FFN54 and FFN246, when measured in the presence of inhibitor, was significantly decreased for both probes (FFN54 and FFN246: $p < 0.0001$, $n = 6$), as observed in representative images B and E, respectively. However, FFN246 has a 58% lower level of non-specific uptake when compared to FFN54 (F, $p < 0.0001$, $n = 6$), highlighted in representative images C and F. Scale bar, 30 μm. H) Signal-to-basal ratio (S/B) of FFN54 and FFN246 uptake at hDAT-EM4, hNET-HEK, and

hSERT-HEK cells after incubation with the compound (5 μM, plate-reader assay) and inhibition with either nomifensine (2 μM, hDAT-EM4 and hNET-HEK) or imipramine (2 μM, hSERT-HEK). FFN246 exhibited a 2.1-fold increase in S/B over FFN54 in HEK cells expressing hSERT ($p < 0.0001$, $n = 6$) FFN246 shows 30% and 40% increased uptake at SERT compared to NET and DAT, respectively ($p < 0.0001$).

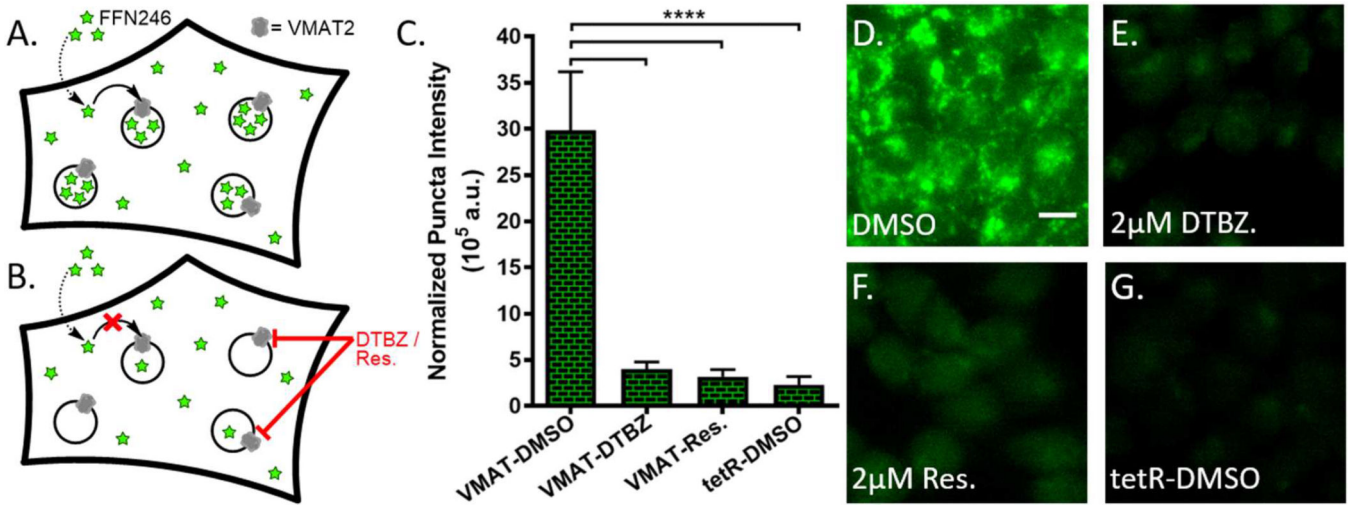

Figure 4.

FFN246 is a VMAT2 substrate. A) Overview schematic of VMAT2-dependent uptake into a HEK cell expressing active vesicular monoamine transporter on intracellular acidic compartments. FFN246 enters the cytosol via passive diffusion, driven by VMAT2-mediated uptake into acidic vesicles, resulting in the bright, punctate staining shown in representative image D. B) Schematic of VMAT2-independent uptake into VMAT2-HEK cells. Inhibition of VMAT2 by dihydrotetrabenazine, DTBZ (E) or reserpine (F) significantly decreased cell uptake of the probe and the punctate staining pattern ($p < 0.0001$, $n = 3$). Null-transfected HEK cells yielded similarly dim, non-punctate labeling (G) ($p < 0.0001$, $n = 3$). C) VMAT2-dependent vesicular loading was quantified as normalized puncta intensity (number of puncta multiplied by average fluorescence of the puncta) normalized to total cell area across the field. Scale bar, 10 μm.

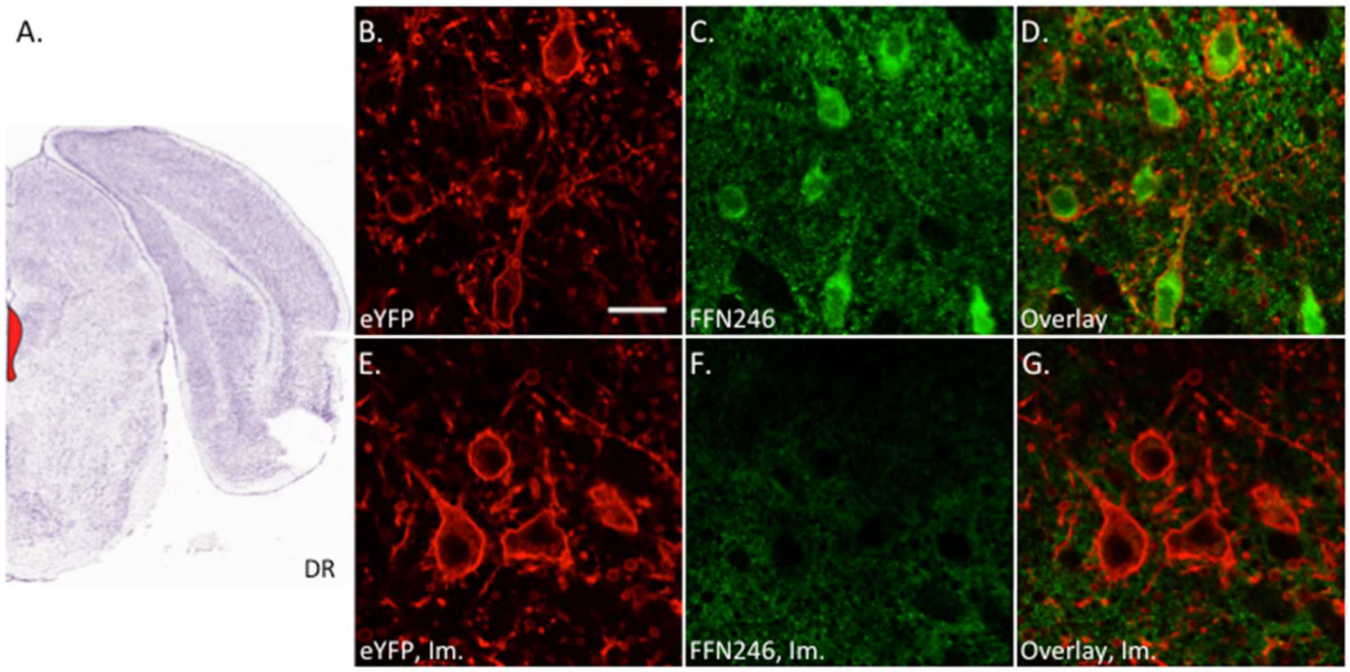

Figure 5.

FFN246 labels 5-HT neurons in the mouse dorsal raphe in an mSERT-dependent manner. A) Mouse brain atlas image highlighting the dorsal raphe (DR) region containing the 5-HT neurons (Bregma: −4.5 mm, Allen Brain Institute).[51] Acute brain slices were collected from Pet1-cre/flox-ChR2-eYFP mice and incubated with FFN246 (20 μM) for 30 min. Uptake of FFN246 (green) in eYFP-positive neurons (red) was counted where FFN signal was greater than two standard deviations above background. 75% of eYFP neurons loaded FFN246 (81/108 neurons from 4 animals). Representative images: eYFP (B), FFN246 (C), and overlay (D). Preincubation with imipramine (Im., 2 μM) completely eliminated FFN246 uptake in 5-HT neurons (0/49 neurons from 3 animals). Representative images of SERT inhibited conditions: eYFP (E), FFN246 (F), and overlay (G). Scale bar, 20 μm.

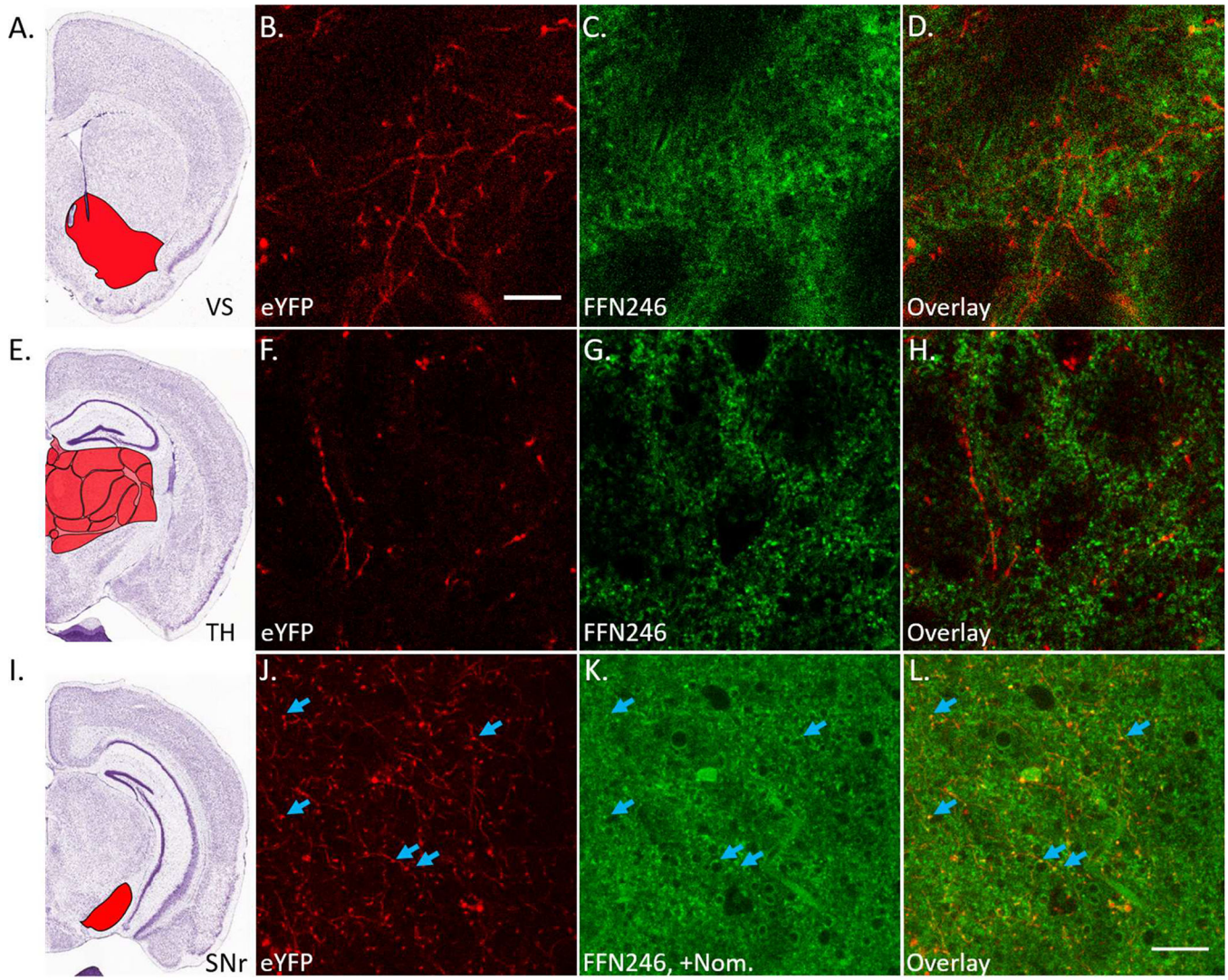

Figure 6.

FFN246 does not significantly label 5-HT axonal projections. A) Mouse brain atlas image highlighting the ventral striatum (VS, Bregma: +0.5 mm, Allen Brain Institute).[51] Brain slices were collected from Pet1-cre/flox-ChR2-eYFP mice and incubated with FFN246 (20 μM) for 30 min. There was no observable colocalization between eYFP (red) and FFN246 (green) in 5-HT neuronal projections (i.e. no FFN signal greater than 2SDs above background in eYFP-positive strands from 3 animals). Representative images: eYFP (B), FFN246 (C), and overlay (D). E) Mouse brain atlas image highlighting the thalamus (TH, Bregma: –1.5 mm).[51] Again, no colocalization between eYFP and FFN246 was observed (3 animals). Representative images: eYFP (F), FFN246 (G), and overlay (H). I) Mouse brain atlas image highlighting the substantia nigra reticulata (SNr, Bregma: −2.5 mm).[51] In this brain region, high FFN246 background staining was also observed even with preincubation of nomifensine (2 μM). However, some puncta colocalized with eYFP axonal signal (blue arrows). Scale bar, 20 μm.